RSC Advances

PAPER

View Article Online
View Journal | View Issue

Cite this: *RSC Adv.*, 2021, **11**, 3655

A quinoxaline-based porous organic polymer containing copper nanoparticles CuNPs@Q-POP as a robust nanocatalyst toward C–N coupling reaction†

Forough Gorginpour, Hassan Zali-Boeini* and Hadi Amiri Rudbari

A novel porous organic polymer (denoted by Q-POP) was successfully fabricated by free-radical copolymerization of allyl-substituted 2,3-di(2-hydroxyphenyl)1,2-dihydroquinoxaline, and divinylbenzene under solvothermal conditions and used as a new platform for immobilization of copper nanoparticles. The CuNPs@Q-POP nanocatalyst was prepared *via* incorporating of $Cu(NO_3)_2$ into the polymeric network, followed by the reduction of Cu^{2+} ion with hydrazine hydrate. The obtained materials were characterized through FT-IR, XRD, N_2 adsorption–desorption isotherms, ICP, TGA, SEM, HR-TEM, EDX, and the single-crystal X-ray crystallography. The results displayed that Q-POP and CuNPs@Q-POP possessed high surface area, hierarchical porosity, and excellent thermal and chemical stability. The as-synthesized catalyst was utilized for the Ullmann C–N coupling reaction of aromatic amines and different aryl halides to prepare various diarylamine derivatives. All types of aryl halides (except aryl fluorides) were screened in the Ullmann C–N coupling reaction with aromatic amines to produce diaryl amines in good to excellent yields (50–98%), and it turned out that aryl iodides have the best results. Besides, due to the strong interactions between CuNPs, N, and O-atoms of quinoxaline moiety existing in the polymeric framework, the copper leaching from the support was not observed. Furthermore, the catalyst was recycled and reused for five consecutive runs without significant activity loss.

Received 22nd December 2020
Accepted 11th January 2021

DOI: 10.1039/d0ra10741g

rsc.li/rsc-advances

1. Introduction

Ullmann coupling reaction is an effective organic synthetic tool to construct carbon–heteroatom bonds leading to valuable compounds with fascinating applications in various fields, including pharmaceutical, biological, and material chemistry.[1–9] In particular, due to the low toxicity and cost of copper-catalyzed Ullmann coupling reactions, they have gained considerable attention compared to other noble metal catalysts.[10–12] However, implementation of the stoichiometric quantities of copper at harsh conditions (>200 °C) and long reaction times are required to run copper-mediated classical Ullmann reactions.[13,14] In this context, diverse copper catalysts with various ligand groups have been developed for carbon–heteroatom bond formation under relatively mild and homogenous conditions.[15–20] Although significant progress has been attained in the homogeneous Cu-catalyzed coupling systems, there are some limitations such as the use of expensive ligands, low recyclability, and metal contamination of products that disqualify them for wide application in industry. In recent years, heterogeneous catalysts are attracting substantial attention due to the role they played for synthetic organic transformations owing to the advantages of good recyclability, reusability, and ease of catalyst separation from the reaction mixture.[21–26] Nevertheless, it is difficult to design and synthesize the heterogeneous catalysts with uniform active centers similar to homogeneous ones. Thus, the development of heterogeneous catalysts, which cover the benefits of both heterogeneous (ease of recyclability) and homogeneous catalysts (easily accessible active sites), have received much attention during recent years.[27–33] This can be done by introducing suitable active centers on porous materials. Indeed, the porosity inside porous materials makes their active centers more accessible and increases reactivity between reactants and active sites. Therefore, these materials can be considered as hosts for guest encapsulation with unique functions such as energy storage, separation, catalysis, sensing, drug delivery, and so on.[34–36] Recently, metal–organic frameworks (MOFs) and covalent organic frameworks (COFs), as porous materials, have been utilized in the above-mentioned fields.[37–45] Despite the extraordinary porosity and large surface areas in MOFs and COFs, they often suffer from low thermal and chemical stability issues under drastic reaction conditions due to weak or reversible

Department of Chemistry, University of Isfahan, 81746-73441, Isfahan, Iran. E-mail: h.zali@chem.ui.ac.ir; Tel: +98-37934925

† Electronic supplementary information (ESI) available. CCDC 1953774. For ESI and crystallographic data in CIF or other electronic format see DOI: 10.1039/d0ra10741g

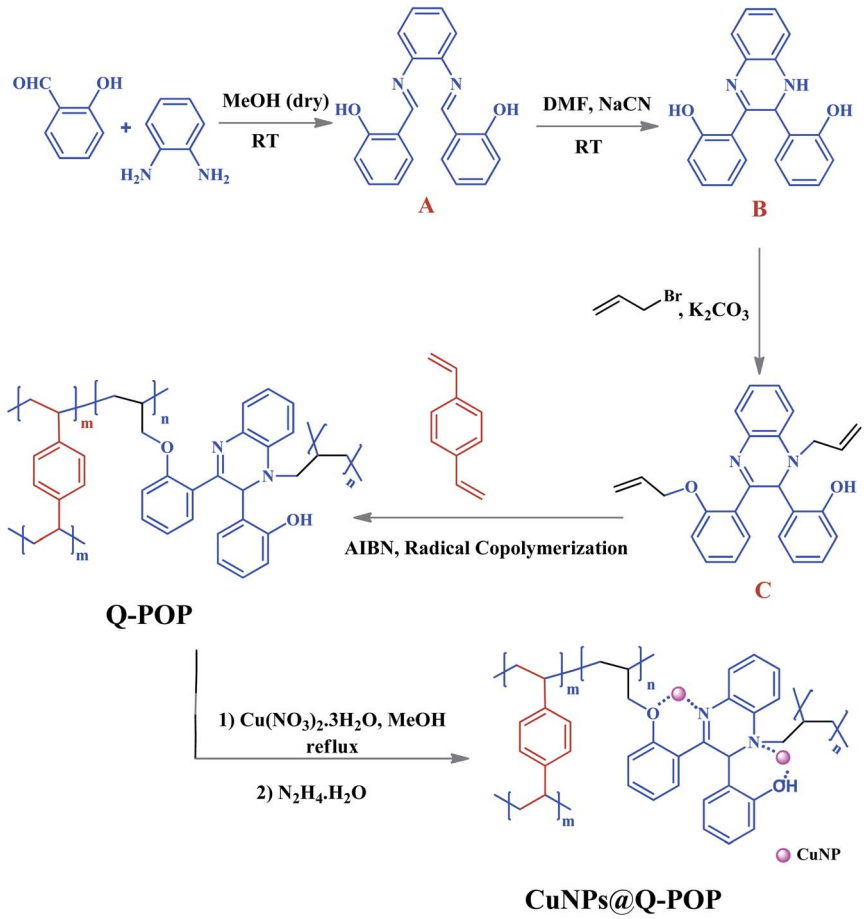

Scheme 1 Synthetic strategy for fabrication of Q-POP and CuNPs@Q-POP.

chemical bonds in their structure.[46] Given these constraints, the constructive units of porous organic polymers (POPs), as superior porous materials, are connected through irreversible covalent bonds. They dedicate permanent porosity, high surface area, and excellent stability toward harsh reaction conditions, which as a result, they have successfully gained wide applications in various fields of science.[47–57] Additionally, numerous organic functional groups can be integrated into the framework of porous organic polymers to act as a proper anchorage to immobilize catalytically active sites and provide heterogeneous catalytic systems. Compared with inorganic porous materials, porous organic polymers that can apply as platforms for heterogeneous catalysis exhibit better catalytic performance. Porous organic polymers contain many organic pores in their structure; therefore, they provide an environment similar to homogeneous conditions. Porous organic polymers can be achieved in different ways,[58–65] but most of the polymerization methods occur in the presence of metals that are costly unfavorable, and environmentally incompatible. Free radical polymerization of organic monomers with double bonds is a suitable strategy for the synthesis of porous organic polymers by taking advantage of low-costs, metal-free, and green strategies. Due to these merits, the preparation of porous organic polymers on a large scale is conceivable and highly desirable. Recently, the free radical strategy was utilized for the polymerization of divinylbenzene to nanoporous polydivinylbenzene under solvothermal conditions, which was used as an adsorbent for removal of organic pollutants from water.[66,67] Based on the high reactivity of organic frameworks in porous polydivinylbenzene, a Schiff base-modified PDVB has

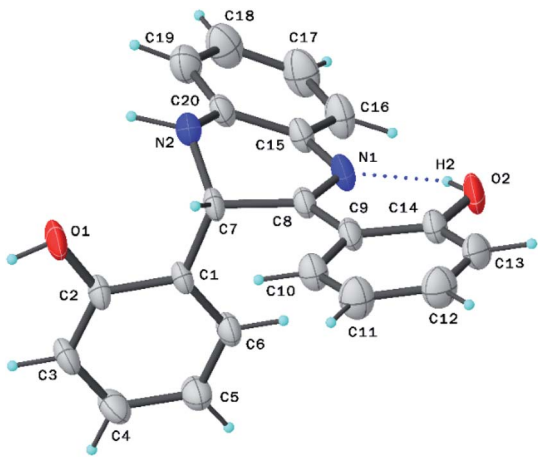

Fig. 1 ORTEP representation of compound B. Displacement ellipsoids are drawn at the 30% probability level and H atoms are shown as small spheres of arbitrary radii. The unit cell contains two independent molecules. Only one molecule is showed for clarity.

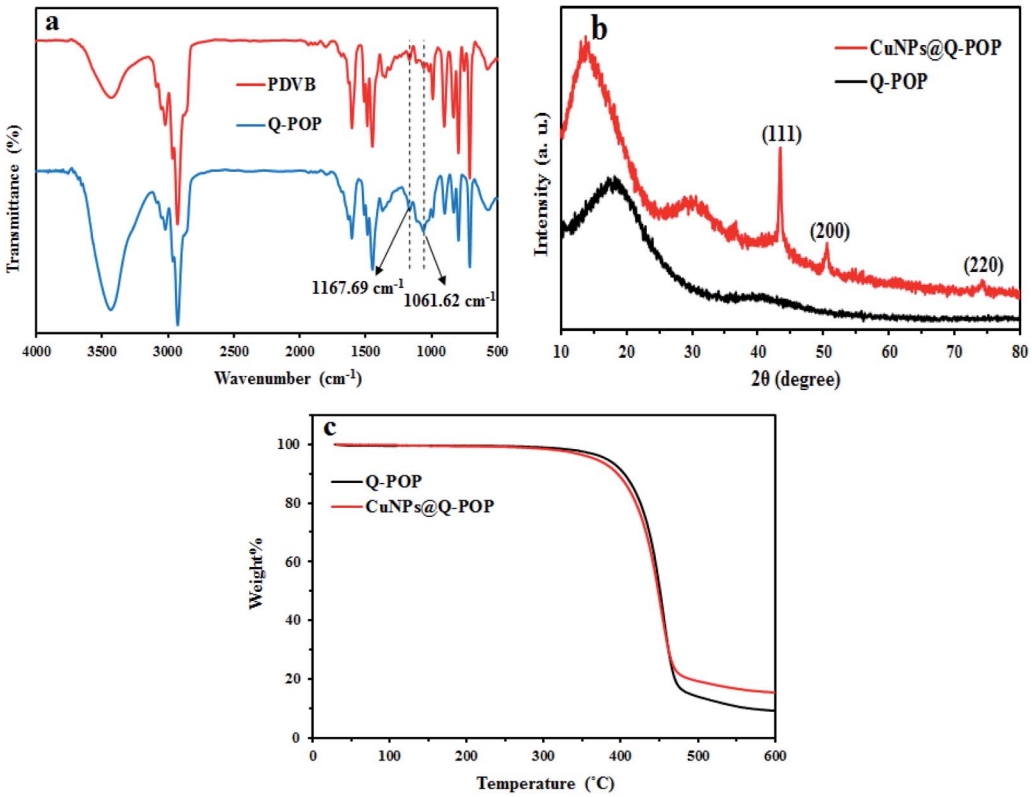

Fig. 2 (a) FT-IR spectra of Q-POP and CuNPs@Q-POP; (b) wide-angle powder XRD patterns of Q-POP and CuNPs@Q-POP; (c) TGA curves of Q-POP and CuNPs@Q-POP.

been prepared through consecutive reactions on the PDVB phenyl ring, in which incorporation of copper cations and complexation leads to PDVB–SB-Cu. The prepared material served as a heterogeneous catalyst for the Ullmann C–O coupling reaction using Cs_2CO_3 as an expensive base in DMSO as the solvent.[68] Despite the fruitful achievements in the context of post-modification of porous organic polymers, difficulties such as reduced surface area and pore blocking during the post-synthetic strategies restrict their widespread use. To this end, a variety of functionalized porous organic polymers have been successfully obtained through pre-functionalized strategies by free radical co-polymerization of functional monomers containing double bonds and divinylbenzene and used for various applications.[69–74] Mondal *et al.* reported the fabrication of a nanoporous polymer DVAC-1 through copolymerization of acrylic acid and divinylbenzene under hydrothermal conditions. The polymer was applied as a support for the deposition of Cu^0 nanoparticles.[75] The resulting Cu^0 supported nanoporous polymer was employed as a heterogeneous nanocatalyst for Ullmann coupling of aryl halides and amines in water.

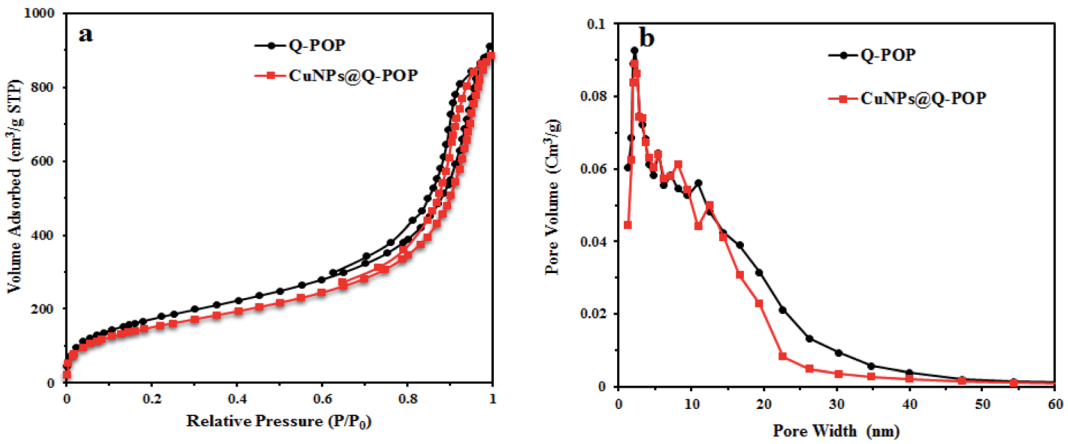

Fig. 3 (a) N_2 sorption isotherms of Q-POP and CuNPs@Q-POP at 77 K; (b) pore size distribution of Q-POP and CuNPs@Q-POP calculated by BJH model.

Table 1 Textural parameters for Q-POP and CuNPs@Q-POP

Material	S_{BET} (m^2 g^{-1})	V_P (cm^3 g^{-1})	D_P (nm)
Q-POP	632.1	1.40	8.9
CuNPs@Q-POP	555.9	1.36	9.8

Notwithstanding the aforementioned developments in the area of POPs, there is still a drastic need to prepare novel POPs containing metal nanoparticles to overcome the previously mentioned limitations and to improve their catalytic activities and recyclability.

Herein, we describe the preparation of a quinoxaline-based porous organic polymer (Q-POP) as a new functionalized mesoporous organic polymer with extraordinary porosity and high stability for immobilization of Cu^0 nanoparticles (CuNPs) and the preparation of CuNPs@Q-POP catalyst (Scheme 1). This novel heterogeneous catalyst demonstrated superior catalytic activity and recyclability for C–N coupling reactions of amines with aryl halides.

2. Results and discussion

2.1 Synthesis of Q-POP mesoporous polymer and CuNPs@Q-POP catalyst

Scheme 1 represents the synthetic pathway of Q-POP and CuNPs@Q-POP. Initially, the bis(salicylidene)-*o*-phenylenediamine (salophen) **A** was prepared through the reaction of *O*-phenylenediamine with salicylaldehyde.[76] Then, 2,3-di(2-hydroxyphenyl) 1,2-dihydroquinoxaline **B** was obtained *via* cyanide-catalyzed cyclization reaction of the salophen under the argon atmosphere. After that, allylation of **B** with allyl bromide produced diallyl derivative of 2,3-di(2-hydroxyphenyl)1,2-dihydro quinoxaline **C** monomer as a new ligand. Subsequently, the desired Q-POP was synthesized by the free-radical copolymerization of ligand **C** and divinylbenzene (DVB) as the cross-linker, using

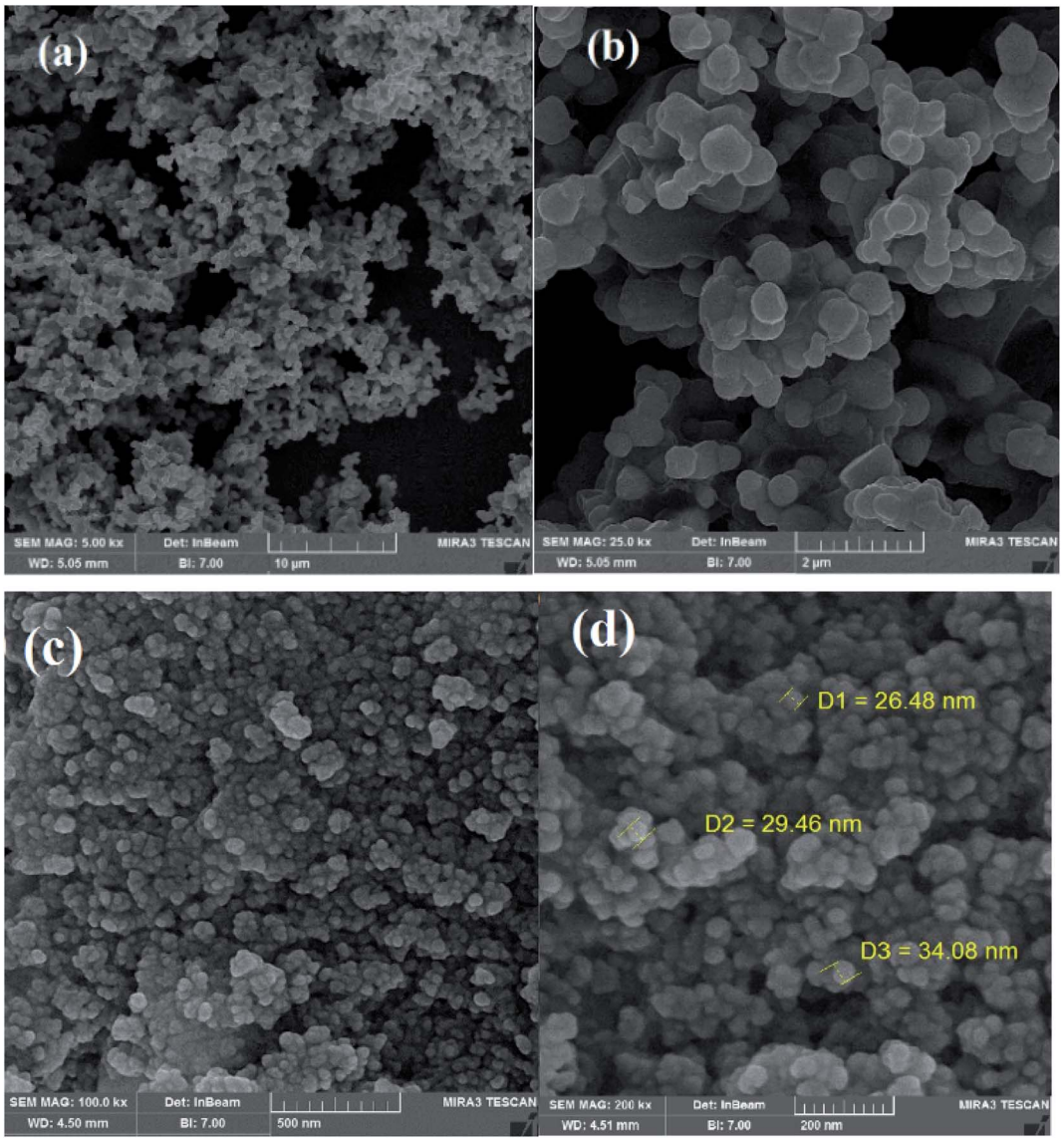

Fig. 4 SEM images of Q-POP (a and b), and CuNPs@Q-POP (c and d).

azobisisobutyronitrile (AIBN) as the radical initiator under solvothermal conditions in the form of yellow solid.

The resultant polymer was not soluble in the common organic solvents such as MeOH, THF, acetone, acetonitrile, DMF, DMSO, and water. Finally, after the treatment of Q-POP with a solution of $Cu(NO_3)_2 \cdot 3H_2O$ in methanol, Cu^{2+}@Q-POP was yielded as a green solid. Indeed, Cu^{2+} ions were immobilized on Q-POP through strong coordination bonds with N and O-atoms present in Q-POP. In the end, CuNPs@Q-POP catalyst was produced as a deep brown solid through the reduction reaction of Cu^{2+} ions to CuNPs using hydrazine hydrate as the reducing agent. The copper content in the CuNPs@Q-POP was determined by inductively coupled plasma (ICP) analysis.

2.2 Characterizations of DHQ ligand, Q-POP polymer, and CuNPs@Q-POP catalyst

The formation of compound **B** as the key structure of the CuNPs@Q-POP was evidenced by its ^1H and ^{13}C NMR spectra and finally confirmed by its X-ray single crystallography analysis (SCXRD, CCDC 1953774, Fig. 1).

Fourier transform infrared spectroscopy (FT-IR) was applied to confirm the ligand C's incorporation in the polymeric network (Fig. 2a). The appearance of extra new bands at 1167.6 cm^{-1} and 1061.6 cm^{-1} assigned to the C–N and C–O stretching vibrations emerged in the Q-POP structure compared with the FT-IR spectra of PDVB, which implies that ligand C was successfully copolymerized with divinylbenzene.

The wide-angle X-ray diffraction (WAXRD) pattern of Q-POP and CuNPs@Q-POP are demonstrated in Fig. 2b. The Q-POP illustrates only one broad diffraction peak, indicating that the as-synthesized polymer possesses an amorphous framework. On the other hand, the XRD pattern of CuNPs@Q-POP displays three additional diffraction peaks at $2\theta = 43.45°$, $50.5°$, and $74.6°$ related to diffractions of the (111), (200), (220) planes, along with one broad peak as compared with Q-POP XRD pattern. These observations validated the existence of CuNPs in CuNPs@Q-POP.

Thermal stabilities of Q-POP and CuNPs@Q-POP were determined by thermal gravimetric analysis (TGA) under an argon atmosphere. Fig. 2c displays that both of these compounds have excellent thermal stabilities up to 300 °C, which could be attributed to the existence of a cross-linked network.

The porosity of Q-POP and CuNPs@Q-POP were measured by nitrogen adsorption and desorption isotherms at 77 K (Fig. 3a). The isotherms for both Q-POP and CuNPs@Q-POP illustrate a slight nitrogen uptake at low relative pressure and a steep uptake with a vivid hysteresis loop at a high relative pressure (*P*/

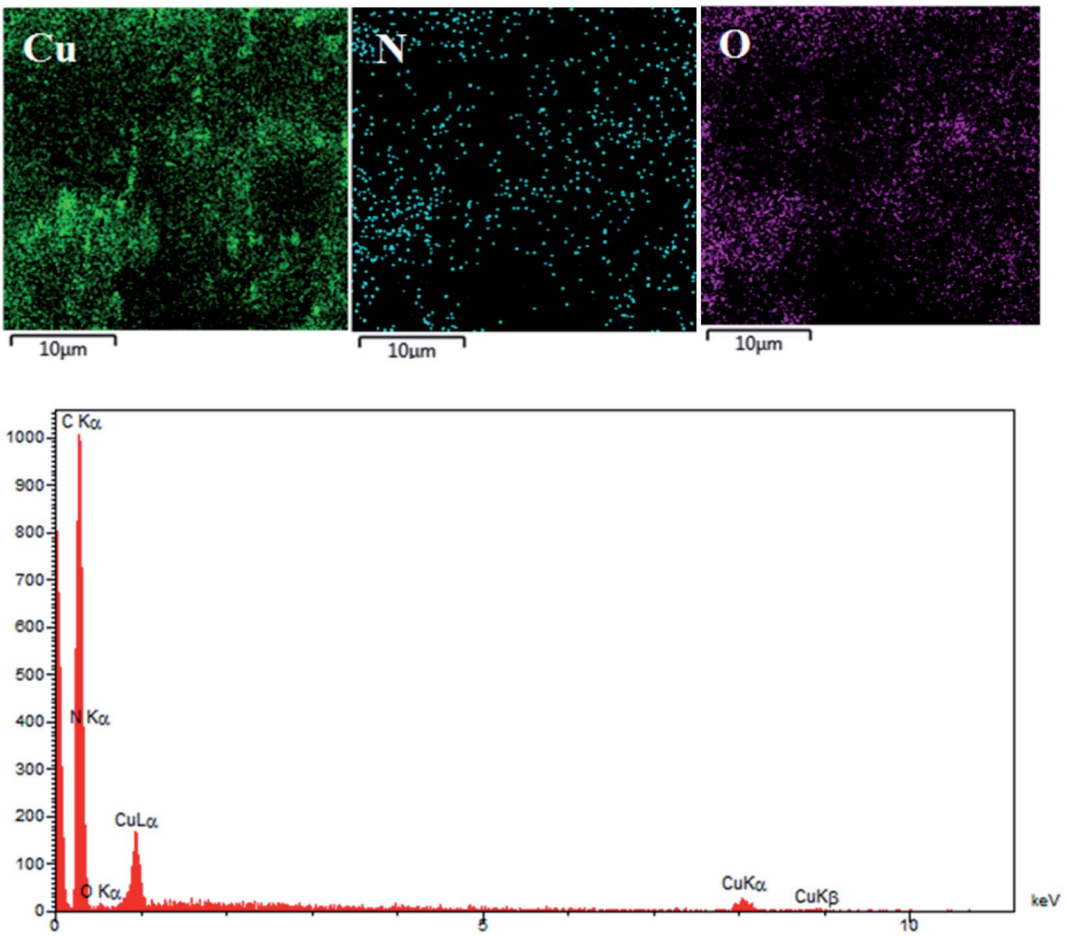

Fig. 5 Elemental mapping and EDX spectrum of N, O, and Cu for CuNPs@Q-POP.

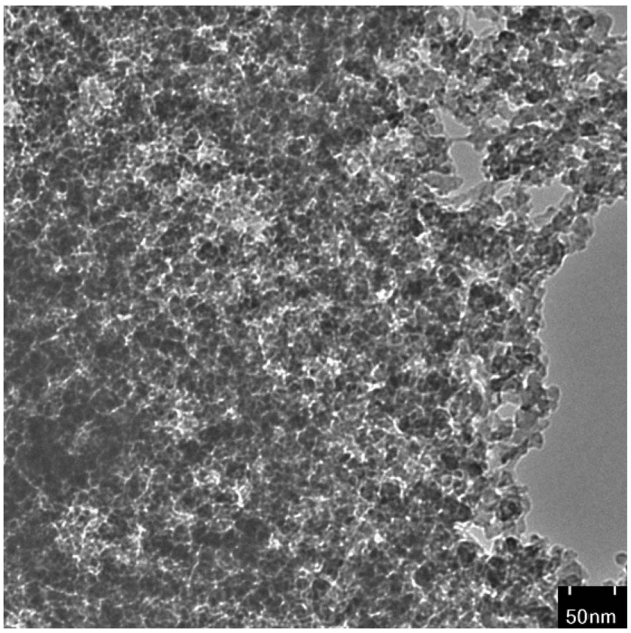

Fig. 6 HR-TEM image of CuNPs@Q-POP.

P_0) of above 0.6, implying type-IV plus type-I isotherm behavior. Therefore, according to the hysteresis loop present in N_2 sorption isotherm and the distribution curves of the pore size using the BJH model (Fig. 3b), both compounds possess hierarchical porosity structure with dominant mesopores, which is highly desirable for promoting the mass transfer of reactants and better catalytic activity.

The BET analysis of Q-POP and CuNPs@Q-POP showed a high surface area 632.1 and 555.9 $m^2\ g^{-1}$, respectively (Table 1).

Fig. 4 displays the scanning electron microscopy (SEM) images of Q-POP and CuNPs@Q-POP. Q-POP shows a spherical morphology with spheres involving tiny irregular particles interconnected with each other. In addition, agglomerated particles and abundant nanoporosity can be seen in the SEM image (Fig. 4a and b). It should be mentioned that SEM images of CuNPs@Q-POP are approximately similar to Q-POP, indicating that morphology is well preserved after Cu loading (Fig. 4c and d).

To evidence the presence of C, O, N and Cu elements in the CuNPs@Q-POP, the energy-dispersive X-ray spectroscopy (EDX) and elemental mapping were carried out (Fig. 5). The elemental mapping images indicate that Cu nanoparticles are rather uniformly dispersed in the porous organic polymer DHQ.

The high-resolution transmission electron microscopy (HR-TEM) is shown in Fig. 6. As revealed in HR-TEM, CuNPs@Q-POP are composed of polymeric frameworks in which the CuNPs are consistently distributed on the Q-POP. Additionally, the HR-TEM image demonstrates that the copper nanoparticles (average size below 6 nm) are well dispersed in the Q-POP texture without the obvious agglomeration.

2.3 N-Arylation of anilines with aryl halides catalyzed by CuNPs@Q-POP

Initially, we surveyed the reaction of aniline with iodobenzene as model substrates for the synthesis of diphenylamine. As indicated in Table 1, a series of parameters, including the influence of Cu loading into Q-POP, amount of catalyst, base type, solvent, temperature, and the reaction time were investigated to find out the optimum reaction conditions. The reaction in the presence of CuNPs@Q-POP (7.3 mol% Cu^0 loading) gave

Table 2 Optimization of various parameters on the cross-coupling of iodobenzene and aniline[a]

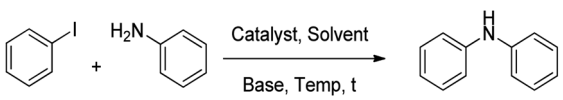

Entry	Catalyst	Cat. (mg)	Solv.	Base	Conv[b]. (%)	Sel[b]. (%)
1	CuNPs@Q-POP (7.3%)	75	PEG-200	K_2CO_3	98	100
2	CuNPs@Q-POP (2.8%)	75	PEG-200	K_2CO_3	98	100
3	CuNPs@Q-POP (2.8%)	50	PEG-200	K_2CO_3	81	100
4	CuNPs@Q-POP (2.8%)	25	PEG-200	K_2CO_3	63	100
5	CuNPs@Q-POP (2.8%)	75	DMF	K_2CO_3	60	100
6[c]	CuNPs@Q-POP (2.8%)	75	H_2O	K_2CO_3	25	100
7	CuNPs@Q-POP (2.8%)	75	Tolu.	K_2CO_3	0	0
8	CuNPs@Q-POP (2.8%)	75	PEG-200	NaOH	70	100
9	CuNPs@Q-POP (2.8%)	75	PEG-200	K_3PO_4	70	100
10	CuNPs@Q-POP (2.8%)	75	PEG-200	Et_3N	30	100
11	CuNPs@Q-POP (2.8%)	75	PEG-200	—	0	0
12	No catalyst	—	PEG-200	K_2CO_3	0	0
13	Q-POP	75	PEG-200	K_2CO_3	0	0
14[d]	CuNPs@Q-POP (2.8%)	75	PEG-200	K_2CO_3	70	100
15[e]	CuNPs@Q-POP (2.8%)	75	PEG-200	K_2CO_3	80	100

[a] Reaction condition: iodobenzene (1 mmol), aniline (1.2 mmol), catalyst, solvent (2.5 mL), base (2 mmol), 110 °C, 24 h. [b] Conversion and selectivity were determined by GC. [c] The reaction was performed in an autoclave. [d] 90 °C. [e] 12 h.

diphenylamine in 98% conversion (Table 2, entry 1). We were surprised by the fact that CuNPs@Q-POP catalyst could also perform the same reaction with almost complete conversion, even when a 2.8 mol% of copper was loaded into Q-POP (Table 2, entry 2). In the reaction of iodobenzene (1 mmol) and aniline (1.2 mmol) when the amount of catalyst was decreased from 75 to 50, and to 25 mg, the reaction conversion was decreased from 98 to 81 and 63% under the same reaction times, respectively (Table 2, entries 3 and 4). Screening of solvents in the reaction revealed that PEG-200 was considered the best solvent for the C–N cross-coupling reaction using CuNPs@Q-POP catalyst. Moreover, the investigations showed that the presence of a base in the reaction mixture was essential, and K_2CO_3 had the highest reaction conversion compared to other bases such as NaOH, K_3PO_4, and Et_3N (Table 2, entries 8–10). We also found that performing the reaction at 110 °C for 24 h without catalyst (Table 2, entry 12) or even in the presence of 75 mg Q-POP (Table 2, entry 13) showed no conversion. Additionally, investigation of reaction temperature on the progress of the reaction indicated that with a decrease in temperature from 110 to 90 °C, the reaction conversion was diminished from 80 to 70% (Table 2, entries 14 and 15). Moreover, our careful studies clarified that the best reaction conversion was achieved after 24 h. Consequently, the best conversion and selectivity for the *N*-arylation of iodobenzene with aniline was obtained using K_2CO_3 as the base, PEG-200 as the solvent, and in the presence of CuNPs@Q-POP (2.8% Cu^0, 75 mg) at 110 °C for 24 h.

Considering the optimized condition, various aniline derivatives bearing both electron-donating and electron-withdrawing substituents were utilized in the coupling reaction with iodobenzene in the presence of CuNPs@Q-POP (2.8% Cu) as the catalytic system. As illustrated in Table 3, anilines possessing electron-donating substituents such as methoxy and/or a methyl group at *para* position produced the corresponding diarylamines in excellent

Table 3 Ullmann *N*-arylation reaction catalyzed by CuNPs@Q-POP(2.8% Cu)[a]

Entry	Aryl halides	Nucleophiles	Products	Conversion[b] (%)	Selectivity[b] (%)
1			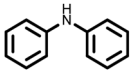	98	100
2		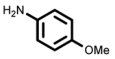	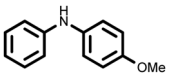	95	100
3		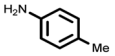	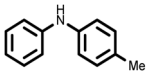	97	100
4		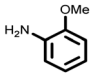	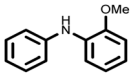	90	100
5		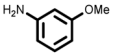	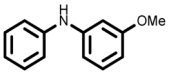	90	100
6		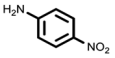	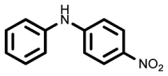	89	80
7		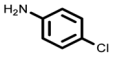	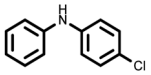	91	85
8			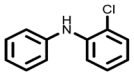	50	100
9			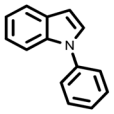	96	100
10			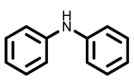	90	100
11			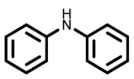	69	100

[a] Reaction condition: aryl halides (1 mmol), amines (1.2 mmol), K_2CO_3 (2 mmol), PEG-200 (2 mL), CuNPs@Q-POP (2.8% Cu, 75 mg), 110 °C, 24 h, under N_2 atmosphere. [b] Conversion and selectivity were determined by GC.

Table 4 Comparison of catalytic performance of CuNPs@Q-POP in the *N*-arylation with the other reported method

Catalyst	Condition	*N*-arylation	Ref.
CuNPs@Q-POP	K_2CO_3, PEG-200, 110 °C	Conversion (98%) Selectivity (100%)	This work
Meso Cu/MnOx	K_2CO_3, DMF, 140 °C	Conversion (5%) Selectivity (90%)	77
CuO/AB	KOtBu, toluene, 180 °C	Conversion (26%)	78
PS-Cu-furfural	Cs_2CO_3, DMSO, *t*-Bu_4NBr, 120 °C	Yield (93%)	79

conversions, and selectivity (Table 3, entries 2 and 3), while anilines with a methoxy group at *ortho* or *meta* position on the phenyl ring gave slightly lower conversions with also 100% selectivity (Table 3, entries 4 and 5). 4-Nitro and 4-chloroaniline showed very good conversions with 80 and 85% selectivity after 24 h, respectively (Table 3, entries 6 and 7). Furthermore, when 2-chloroaniline was applied as substrate, the conversion rate was 50% and the desired product was afforded with complete selectivity (Table 3, entry 8). Indole as a heterocyclic amine was also coupled well with iodobenzene to generate an *N*-arylated product with excellent selectivity (100%, Table 3, entry 9). The coupling reaction of aniline with bromobenzene and chlorobenzene was also successful, with conversion rates of 90 and 69%, respectively, along with 100% selectivity for both of them (Table 3, entries 10 and 11).

2.4 The comparison of our method with some reported method in the literature

In Table 4, the catalytic activity of our present catalytic system with various reported heterogeneous catalysts in the *N*-arylation of iodobenzene with aniline is compared.[77–79] Our synthesized CuNPs@Q-POP catalyst demonstrates better or comparable performance over reported catalysts. It is more likely, high catalytic activity and durability of our catalyst can be ascribed to the extraordinary stability of the polymeric network as a support along with large pore size playing the role of nanoreactor and the facilitated diffusion of reactants inside the polymeric network of catalyst. On the other hand, the *N*-arylation of iodobenzene with aniline occurred in PEG-200 as a safe and eco-friendly solvent over our CuNPs@Q-POP catalyst.

To check the recyclability of the catalyst, CuNPs@Q-POP as a solid was separated from the reaction mixture by filtration and then washed with water, ethyl acetate, and methanol, respectively, and dried under vacuum. Ultimately, the isolated and refined catalyst was applied for numerous consecutive recycle runs under the optimized reaction conditions in the *N*-arylation of iodobenzene with aniline. It was found that the recycled catalyst for the C–N cross-coupling reaction could be reused five times without appreciable reduction in the conversion rate and selectivity (Fig. 7). Wide-angle X-ray diffraction (WAXRD) patterns of the reused CuNPs@Q-POP after the fifth run were similar to the fresh nanocatalyst (Fig. S1†). The SEM images indicate that the morphology of CuNPs@Q-POP is well maintained after five runs (Fig. S2†). Furthermore, ICP analysis reveals that the reused CuNPs@Q-POP possesses Cu content of 2.74 mol%, which is close to fresh CuNPs@Q-POP (2.8 mol%). To confirm that the CuNPs@Q-POP is a heterogeneous catalyst, Hg poisoning test using an excess amount of Hg^0 was performed. When the optimal conditions was used to perform the reaction of aniline and iodobenzene (entry 1, Table 3) using CuNPs@Q-POP catalyst in the presence of excess amount of metallic mercury, the reaction conversion was dropped drastically from 100 to <10% as a result of Hg–Cu amalgam formation. This clearly approve that, the CuNPs@Q-POP is heterogeneous. A hot filtration test was also accomplished to further survey the heterogeneous nature of separated CuNPs@Q-POP. In the *N*-arylation of iodobenzene with aniline under optimized conditions, the catalyst was filtered from the reaction mixture after 8 h (57% conversion). Then, the reaction of the filtrate was further continued at the same reaction conditions for an additional 16 h. No changes in conversion and selectivity were observed after removing the catalyst. According to the results of this experiment, we concluded that there were no copper nanoparticles in the filtrate and the atomic absorption spectroscopy confirmed it. Nevertheless, a closer investigation of the used catalyst by ICP showed that a very little leaching of the copper nanoparticles (0.7%) was seen in the solution and the final content of copper in the CuNPs@Q-POP catalyst was 2.78%. High catalyst stability and low copper leaching can be attributed to the strong chemical interaction between CuNPs and N and O binding sites in Q moiety present in the polymer network.

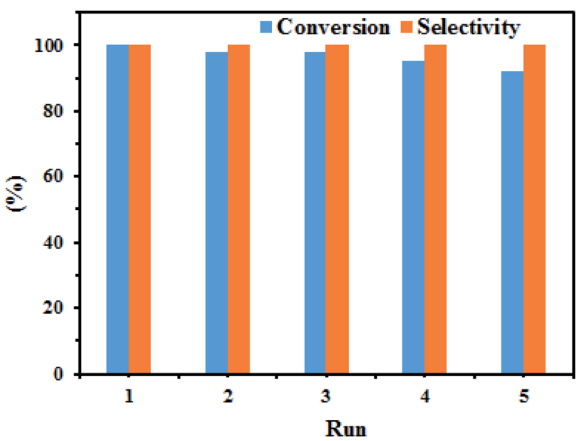

Fig. 7 Recyclability of CuNPs@Q-POP Ullmann *N*-arylation. Reaction conditions for cross-coupling of iodobenzene and aniline: iodobenzene (1 mmol), aniline (1.2 mmol), K_2CO_3 (2 mmol), PEG-200 (2 mL), CuNPs@Q-POP (2.8% Cu, 75 mg), 110 °C, 24 h, under N_2 atmosphere.

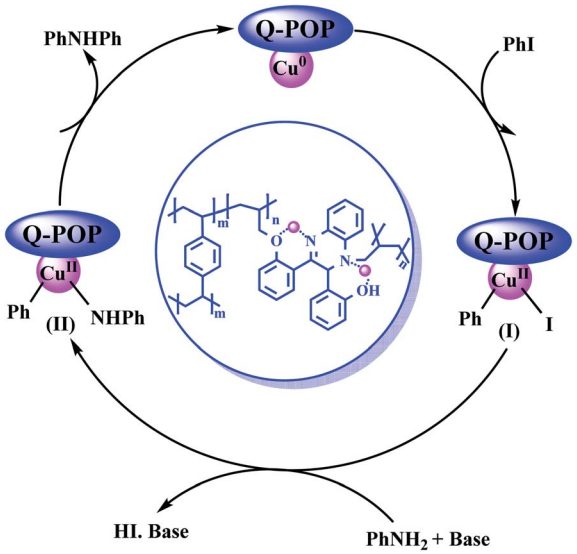

Scheme 2 The plausible reaction mechanism for the *N*-arylation of iodobenzene with aniline catalysed by CuNPs@Q-POP.

The feasibility of a multi-gram scale synthesis was also checked for the catalyst. When the C–N coupling reaction of aniline was performed with iodobenzene in a 50 mmol scale, the resulting diphenylamine compounds were produced with a nearly complete conversion.

A plausible mechanism for the *N*-arylation of iodobenzene with aniline is shown in Scheme 2. The catalytic cycle commences with the oxidative addition of iodobenzene to the Cu^0 nanoparticles of CuNPs@Q-POP to give the intermediate (I). Subsequently, the intermediate (I) is reacted with the nucleophile to form the intermediate (II) followed by reductive elimination to generate the desired product.

3. Conclusion

In summary, we synthesized Q-POP as a new porous organic polymer through a facile metal-free, environmentally friendly, and efficient free-radical copolymerization of allyl-substituted 2,3-di(2-hydroxyphenyl)1,2-dihydroquinoxaline, and divinylbenzene under solvothermal conditions, followed by treating with $Cu(NO_3)_2 \cdot 3H_2O$ and reduction with hydrazine hydrate to produce CuNPs@Q-POP. The resultant Q-POP polymer and CuNPs@Q-POP catalyst showed high surface area, large pore volume, hierarchical porosity, and astonishing thermal stability. The CuNPs@Q-POP was employed as an efficient heterogeneous catalyst for the *N*-arylation reaction of aryl halides with amines. Indeed, the anchoring of quinoxaline moiety to a porous polymeric network provided excellent confinement that stabilized CuNPs through coordination and/or electrostatic interactions with quinoxaline moiety present in the POP skeleton. Furthermore, the hierarchical porosity in CuNPs@Q-POP enhanced the diffusion of reactants and thus resulted in high catalytic activity. Additionally, the catalyst could be readily separated and recycled from the reaction mixture with no noticeable loss of catalytic activity after recycling five times. We found that the as-synthesized CuNPs@Q-POP catalyst might be used in other synthetic transformations. Meanwhile, Q-POP polymer has the potential to be used in many other research fields such as the light-emissive layer in OLEDs (due to its intense fluorescence), making different catalysts with changing copper with other metals, removing of organic chemical pollutants, and toxic heavy metal ions from wastewater. The aforementioned studies are currently underway in our laboratory.

Conflicts of interest

Authors hereby confirm that there is no competing interests to declare.

Acknowledgements

The authors are grateful to the University of Isfahan research council for providing instrumental facilities and partial financial support for this work.

References

1 M. Negwar, in *Organic-Chemical Drugs and their Synonyms: (An International Survey)*, Akademic, Berlin, 7th edn, 1994.
2 M. Liang and J. Chen, *Chem. Soc. Rev.*, 2013, **42**, 3453–3488.
3 S.-M. Yang, Z.-N. Huang, Z.-S. Zhou, J. Hou, M.-Y. Zheng, L.-J. Wang, Y. Jiang, X.-Y. Zhou, Q.-Y. Chen, S.-H. Li and F.-N. Li, *Arch. Pharmacal Res.*, 2015, **38**, 1761–1773.
4 R. K. V. Devambatla, O. A. Namjoshi, S. Choudhary, E. Hamel, C. V. Shaffer, C. C. Rohena, S. L. Mooberry and A. Gangjee, *J. Med. Chem.*, 2016, **59**, 5752–5765.
5 S. Yang, C. Wu, H. Zhou, Y. Yang, Y. Zhao, C. Wang, W. Yang and J. Xu, *Adv. Synth. Catal.*, 2013, **355**, 53–58.
6 J. Haumesser, A. M. V. M. Pereira, J.-P. Gisselbrecht, K. Merahi, S. Choua, J. Weiss, J. A. S. Cavaleiro and R. Ruppert, *Org. Lett.*, 2013, **15**, 6282–6285.
7 J. Y. Hwang, T. Kawasuji, D. J. Lowes, J. A. Clark, M. C. Connelly, F. Zhu, W. A. Guiguemde, M. S. Sigal, E. B. Wilson, J. L. DeRisi and R. K. Guy, *J. Med. Chem.*, 2011, **54**, 7084–7093.
8 M. Q. Salih and C. M. Beaudry, *Org. Lett.*, 2013, **15**, 4540–4543.
9 M.-J. R. P. Queiroz, D. Peixoto, R. C. Calhelha, P. Soares, T. dos Santos, R. T. Lima, J. F. Campos, R. M. V. Abreu, I. C. F. R. Ferreira and M. H. Vasconcelos, *Eur. J. Med. Chem.*, 2013, **69**, 855–862.
10 X.-X. Guo, D.-W. Gu, Z. Wu and W. Zhang, *Chem. Rev.*, 2015, **115**, 1622–1651.
11 C. Sambiagio, S. P. Marsden, A. J. Blacker and P. C. McGowan, *Chem. Soc. Rev.*, 2014, **43**, 3525–3550.
12 S. Benyahya, F. Monnier, M. Taillefer, M. W. C. Man, C. Bied and F. Ouazzani, *Adv. Synth. Catal.*, 2008, **350**, 2205–2208.
13 R. Frlan and D. Kikelj, *Synthesis*, 2006, **14**, 2271–2285.
14 F. Ullmann and J. Bielecki, *Ber. Dtsch. Chem. Ges.*, 1901, **34**, 2174–2185.

15 M. Wolter, G. Nordmann, G. E. Job and S. L. Buchwald, *Org. Lett.*, 2002, **4**, 973–976.
16 S. Benyahya, F. Monnier, M. W. C. Man, C. Bied, F. Ouazzani and M. Taillefer, *Green Chem.*, 2009, **11**, 1121–1123.
17 D. Kundu, S. Bhadra, N. Mukherjee, B. Sreedhar and B. C. Ranu, *Chem.–Eur. J.*, 2013, **19**, 15759–15768.
18 A. C. Bissember, R. J. Lundgren, S. E. Creutz, J. C. Peters and G. C. Fu, *Angew. Chem., Int. Ed.*, 2013, **52**, 5129–5133.
19 A. Ouali, J.-F. Spindler, A. Jutand and M. Taillefer, *Adv. Synth. Catal.*, 2007, **349**, 1906–1916.
20 D. Maiti and S. L. Buchwald, *J. Am. Chem. Soc.*, 2009, **131**, 17423–17429.
21 B. Sels, D. Devos, M. Buntinx, F. Pierard, A. K. Mesmaeker and P. A. Jacobs, *Nature*, 1999, **400**, 855–857.
22 C. Coperet, M. Chabanas, R. P. Saint-Arroman and J.-M. Basset, *Angew. Chem., Int. Ed.*, 2003, **42**, 156–181.
23 R. A. Sheldon, *Green Chem.*, 2005, **7**, 267–278.
24 A. Corma and H. Garcia, *Chem. Rev.*, 2003, **103**, 4307–4366.
25 J. M. Thomas, R. Raja and D. W. Lewis, *Angew. Chem., Int. Ed.*, 2005, **44**, 6456–6482.
26 S. Kramer, F. Hejjo, K. H. Rasmussen and S. Kegnæs, *ACS Catal.*, 2018, **8**, 754–759.
27 D. J. Cole-Hamilton, *Science*, 2003, **299**, 1702–1706.
28 D. Astruc, F. Lu and J. R. Aranzaes, *Angew. Chem., Int. Ed.*, 2005, **44**, 7852–7872.
29 D. E. De Vos, M. Dams, B. F. Sels and P. Jacobs, *Chem. Rev.*, 2002, **102**, 3615–3640.
30 V. K. Dioumaev and R. M. Bullock, *Nature*, 2000, **424**, 530–532.
31 C. A. Witham, W. Huang, C.-K. Tsung, J. N. Kuhn, G. A. Somorjai and F. D. Toste, *Nat. Chem.*, 2009, **2**, 36–41.
32 D. S. Su, S. Perathoner and G. Centi, *Chem. Rev.*, 2013, **113**, 5782–5816.
33 F. Wang, J. Mielby, F. H. Richter, G. Wang, G. Prieto, T. Kasama, C. Weidenthaler, H. J. Bongard, S. Kegnæs, A. Fürstner and F. Schüth, *Angew. Chem., Int. Ed.*, 2013, **53**, 8645–8648.
34 M. E. Davis, *Nature*, 2002, **417**, 813–821.
35 A. Thomas, *Angew. Chem., Int. Ed.*, 2010, **49**, 8328–8344.
36 P. Kaur, J. T. Hupp and S. T. Nguyen, *ACS Catal.*, 2011, **1**, 819–835.
37 P. Horcajada, R. Gref, T. Baati, P. K. Allan, G. Maurin, P. Couvreur, G. Férey, R. E. Morris and C. Serre, *Chem. Soc. Rev.*, 2012, **112**, 1232–1268.
38 C. J. Doonan, D. J. Tranchemontagne, T. G. Glover, J. R. Hunt and O. M. Yaghi, *Nat. Chem.*, 2010, **2**, 235–238.
39 W.-Y. Gao, M. Chrzanowski and S. Ma, *Chem. Soc. Rev.*, 2014, **43**, 5841–5866.
40 J. Liu, L. Chen, H. Cui, J. Zhang, L. Zhang and C.-Y. Su, *Chem. Soc. Rev.*, 2014, **43**, 6011–6061.
41 Y. Zeng, R. Zou and Y. Zhao, *Adv. Mater.*, 2016, **28**, 2855–2873.
42 H. Xu, J. Gao and D. Jiang, *Nat. Chem.*, 2015, **7**, 905–912.
43 A. I. Cooper, *Adv. Mater.*, 2009, **21**, 1291–1295.
44 L. E. Kreno, K. Leong, O. K. Farha, M. Allendorf, R. P. VanDuyne and J. T. Hupp, *Chem. Rev.*, 2012, **112**, 1105–1125.
45 X. Zhu, C. Tian, S. Mahurin, S.-H. Chai, C. Wang, S. Brown, G. M. Veith, H. Luo, H. Liu and S. Dai, *J. Am. Chem. Soc.*, 2012, **134**, 10478–10484.
46 J. J. Low, A. I. Benin, P. Jakubczak, J. F. Abrahamian, S. A. Faheem and R. R. Willis, *J. Am. Chem. Soc.*, 2009, **131**, 15834–15842.
47 Y. Zhang, B. Li and S. Ma, *Chem. Commun.*, 2014, **50**, 8507–8510.
48 W. Wang, A. Zheng, P. Zhao, C. Xia and F. Li, *ACS Catal.*, 2014, **4**, 321–327.
49 W. Zhang, B. Aguila and S. Ma, *J. Mater. Chem. A*, 2017, **5**, 8795–8824.
50 Y. Xu, S. Jin, H. Xu, A. Nagai and D. Jiang, *Chem. Soc. Rev.*, 2013, **42**, 8012–8031.
51 B. Li, Y. Zhang, D. Ma, Z. Shi and S. Ma, *Nat. Commun.*, 2014, **5**, 5537–5543.
52 Y. Zhang and S. N. Riduan, *Chem. Soc. Rev.*, 2012, **41**, 2083–2094.
53 Y. Zhu, H. Long and W. Zhang, *Chem. Mater.*, 2013, **25**, 1630–1635.
54 Q. Chen, M. Luo, P. Hammershøj, D. Zhou, Y. Han, B. W. Laursen, C.-G. Yan and B.-H. Han, *J. Am. Chem. Soc.*, 2012, **134**, 6084–6087.
55 Z. Li, H. Li, H. Xia, X. Ding, X. Luo, X. Liu and Y. Mu, *Chem.–Eur. J.*, 2015, **21**, 17355–17362.
56 Q. Sun, Z. Dai, X. Meng and F.-S. Xiao, *Chem. Soc. Rev.*, 2015, **44**, 6018–6034.
57 L. Tan and B. Tan, *Chem. Soc. Rev.*, 2017, **46**, 3322–3356.
58 T. Ben, H. Ren, S. Ma, D. Cao, J. Lan, X. Jing, W. Wang, J. Xu, F. Deng, J. M. Simmons, S. Qiu and G. Zhu, *Angew. Chem., Int. Ed.*, 2009, **48**, 9457–9460.
59 L. Li, H. Zhao, J. Wang and R. Wang, *ACS Nano*, 2014, **8**, 5352–5364.
60 B. Li, Z. Guan, W. Wang, X. Yang, J. Hu, B. Tan and T. Li, *Adv. Mater.*, 2012, **24**, 3390–3395.
61 B. G. Hauser, O. K. Farha, J. Exley and J. T. Hupp, *Chem. Mater.*, 2013, **25**, 12–16.
62 Y. Zhu, Y. Ji, D. Wang, Y. Zhang, H. Tang, X. Jia, M. Song, G. Yu and G. Kuang, *J. Mater. Chem. A*, 2017, **5**, 6622–6629.
63 Z.-A. Qiao, S.-H. Chai, K. Nelson, Z. Bi, J. Chen, S. M. Mahurin, X. Zhu and S. Dai, *Nat. Commun.*, 2014, **5**, 3705–3712.
64 J. Schmidt, J. Weber, J. D. Epping, M. Antonietti and A. Thomas, *Adv. Mater.*, 2009, **21**, 702–705.
65 L. Chen, Y. Yang and D. Jiang, *J. Am. Chem. Soc.*, 2012, **132**, 9138–9143.
66 Y. Zhang, S. Wei, F. Liu, Y. Du, S. Liu, Y. Ji, T. Yokoi, T. Tatsumi and F.-S. Xiao, *Nano Today*, 2009, **4**, 135–142.
67 Y. Zhang, J. N. Wang, Y. He, Y. Y. He, B. B. Xu, S. Wei and F.-S. Xiao, *Langmuir*, 2011, **27**, 12585–12590.
68 L. Wang, J. Zhang, J. Sun, L. Zhu, H. Zhang, F. Liu, D. Zheng, X. Meng, X. Shi and F.-S. Xiao, *ChemCatChem*, 2013, **5**, 1606–1613.
69 F. Liu, W. Kong, C. Qi, L. Zhu and F.-S. Xiao, *ACS Catal.*, 2012, **2**, 565–572.
70 Z. Guo, X. Cai, J. Xie, X. Wang, Y. Zhou and J. Wang, *ACS Appl. Mater. Interfaces*, 2016, **8**, 12812–12821.

71 H. Gao, L. Ding, W. Li, G. Ma, H. Bai and L. Li, *ACS Macro Lett.*, 2016, **5**, 377–381.
72 Q. Sun, X. Meng, X. Liu, X. Zhang, Y. Yang, Q. Yang and F.-S. Xiao, *Chem. Commun.*, 2012, **48**, 10505–10507.
73 Q. Sun, Z. Lv, Y. Du, Q. Wu, L. Wang, L. Zhu, X. Meng, W. Chen and F.-S. Xiao, *Chem.–Asian J.*, 2013, **8**, 2822–2827.
74 H. Wang, Y. Shi, M. Haruta and J. Huang, *Appl. Catal., A*, 2017, **536**, 27–34.
75 J. Mondal, A. Biswas, S. Chiba and Y. Zhao, *Sci. Rep.*, 2015, **5**, 8294.
76 B. J. E. Reich, A. K. Justice, B. T. Beckstead, J. H. Reibenspies and S. A. Miller, *J. Org. Chem.*, 2004, **69**, 1357–1359.
77 K. Mullick, S. Biswas, C. Kim, R. Ramprasad, A. M. Angeles-Boza and S. L. Suib, *Inorg. Chem.*, 2017, **56**, 10290–10297.
78 A. Y. Kim, H. J. Lee, J. C. Park, H. Kang, H. Yang, H. Song and K. H. Park, *Molecules*, 2009, **14**, 5169–5178.
79 S. k. M. Islam, N. Salam, P. Mondal, A. S. Roy, K. Ghosh and K. A. Tuhina, *J. Mol. Catal. A: Chem.*, 2014, **387**, 7–19.